

Biosensors based on surface plasmon-enhanced fluorescence spectroscopy (Review)

Jakub Dostálek^{a)} and Wolfgang Knoll

Max Planck Institute for Polymer Research, Ackermannweg 10, 55128 Mainz, Germany

(Received 2 May 2008; accepted 11 July 2008; published 16 January 2009)

The implementation of surface plasmon-enhanced fluorescence spectroscopy (SPFS) to surface plasmon resonance (SPR) biosensors enables increasing their sensitivity by several orders of magnitude. In SPR-based biosensors, surface plasmons probe the binding of target molecules contained in a liquid sample by their affinity partners attached to a metallic sensor surface. SPR biosensors relying on the detection of refractive index changes allow for direct observation of the binding of large and medium size molecules that produces sufficiently large refractive index changes. In SPR biosensors exploiting SPFS, the capture of fluorophore-labeled molecules to the sensor surface is observed by the detection of fluorescence light emitted from the surface. This technique takes advantage of the enhanced intensity of electromagnetic field accompanied with the resonant excitation of surface plasmons. The interaction with surface plasmons can greatly increase the measured fluorescence signal through enhancing the excitation rate of fluorophores and by more efficient collecting of fluorescence light. SPFS-based biosensors were shown to enable the analysis of samples with extremely low analyte concentrations and the detection of small molecules. In this review, we describe the fundamental principles, implementations, and current state of the art applications of SPFS biosensors. This review focuses on SPFS-based biosensors employing the excitation of surface plasmons on continuous metal-dielectric interfaces. © 2008 American Vacuum Society. [DOI: 10.1116/1.2994688]

I. INTRODUCTION

Biosensors based on surface plasmon resonance (SPR) are optical devices which rely on the excitation of surface plasmons (SPs)—electromagnetic waves guided at the interface between a metal and a dielectric. In these devices, surface plasmons are used to probe the binding of target molecules contained in a liquid sample to their affinity partners anchored to the metallic sensor surface. The capture of target molecules on the surface leads to a local increase in the refractive index which can be directly measured from induced shift in the SPR angle of incidence or wavelength. This approach offers the advantage of label-free detection and it found numerous applications in the analysis of biomolecular interactions and for the detection of chemical and biological species.^{1–3}

However, the detection of small molecules and the analysis of samples with very low concentrations of analytes remain a challenge for SPR biosensors. In order to increase their sensitivity, research has been carried out to improve the resolution of SPR-based measurement of refractive index changes^{4,5} as well as toward the amplification of the sensor response. Over the past years, amplification approaches exploiting enzymatic reactions and labeling with gold nanoparticles and chromophores were developed for SPR biosensors pushing their detection limit by several orders of magnitude.^{6–11} For instance, direct measurement of binding induced refractive index changes enables the detection of

DNA hybridization at concentrations 0.1 nM.^{12,13} The refractive index changes were shown to be dramatically increased by employing gold nanoparticle labels which allowed for the detection of DNA hybridization at concentrations of as low as 10 pM.⁶ By combining the gold nanoparticle labels with SP-enhanced diffraction on periodically patterned metallic surface, sensing of RNA at 10 fM levels was achieved.⁷ The same limit of detection was achieved for the detection of RNA by using gold nanoparticle labels and polyadenyl enzyme amplification.¹¹ The detection of DNA at concentrations reaching 100 fM level through a chromophore-labeling and surface plasmon-enhanced fluorescence spectroscopy (SPFS) was reported.¹⁴

In this review, we summarize the current state of the art SPR-based biosensors relying on SPFS. This method combines SPR biosensing with fluorescence spectroscopy which provides a novel platform for highly sensitive observation of biomolecular binding events.^{9,15} Compared to other techniques utilizing fluorescence spectroscopy,^{16–18} the SPFS method offers a greatly increased fluorescence signal owing to the surface plasmon-enhanced intensity of the electromagnetic field on the sensor surface. Further, we focus on SPFS biosensors that exploit SPs propagating along continuous metallic films. Reviews on the fluorescence spectroscopy techniques utilizing localized surface plasmons on nanostructured metallic materials can be found elsewhere.^{19,20}

II. SURFACE PLASMONS ON THIN METALLIC FILMS

SPs are optical waves that originate from coupled collective oscillations of the electron plasma and the associated

^{a)}Author to whom correspondence should be addressed; electronic mail: dostalek@mpip-mainz.mpg.de

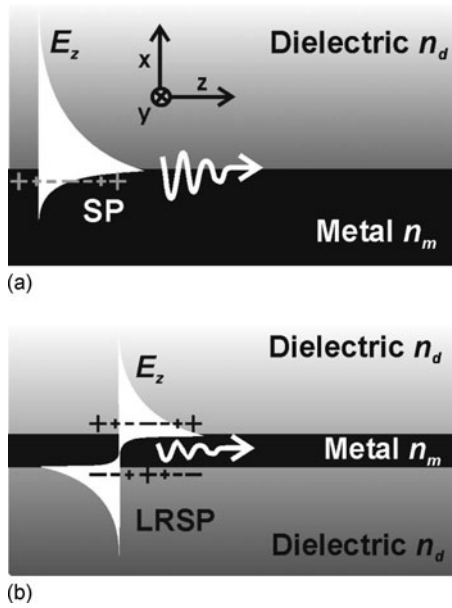


FIG. 1. (a) SP propagating on a metal-dielectric interface and (b) LRSP guided along a thin metal film embedded between dielectrics with identical refractive index.

electromagnetic field on a metallic surface,²¹ see Fig. 1(a). Along an interface between a semi-infinite metal and a dielectric, SPs propagate with the complex propagation constant β described as

$$\beta = k_0 \sqrt{\frac{n_m^2 n_d^2}{n_m^2 + n_d^2}}, \quad (1)$$

where $k_0 = 2\pi/\lambda$ is the wave vector of light in vacuum, λ is the wavelength, n_d is the refractive index of the dielectric, and n_m is the (complex) refractive index of the metal. The electromagnetic field of SP is transverse magnetic (TM) polarized and decays exponentially from the metal-dielectric interface. Typically, the penetration depth of SP into the dielectric is several hundreds of nanometers, whereas the penetration depth into the metal is an order of magnitude lower. Due to the losses within a metal, the energy of SP wave dissipates while it propagates along the metallic surface. For instance, on a gold-air interface the propagation length of SP reaches $56 \mu\text{m}$ for the wavelength $\lambda = 0.85 \mu\text{m}$ and $8 \mu\text{m}$ for the wavelength $\lambda = 0.633 \mu\text{m}$. The propagation length of SPs can be increased by more than an order of magnitude by coupling of two SPs propagating on opposite interfaces of a thin metal film surrounded by dielectrics with identical refractive indices n_d . Such a symmetrical refractive index structure supports a special SP mode with an antisymmetric profile of the electric intensity field component that is parallel to the interface, see Fig. 1(b). This mode is referred to as long range SP (LRSP) (Ref. 22) and it obeys the following dispersion relation:

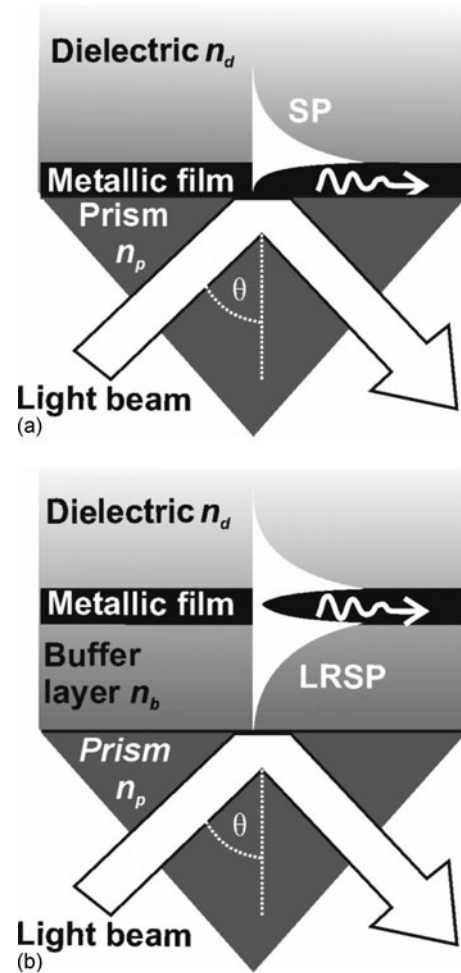


FIG. 2. Prism couplers utilizing the ATR method for the excitation of (a) SPs and (b) LRSPs.

$$\tan(\kappa d_m) = \frac{2\gamma_m^2 / \kappa n_d^2}{1 - (\gamma_m^2 / \kappa n_d^2)^2}, \quad (2)$$

where d_m is the thickness of the metal film and $\kappa = (k_0^2 n_m^2 - \beta^2)^{1/2}$ and $\gamma = (\beta^2 - k_0^2 n_d^2)^{1/2}$ are the transverse propagation constants in the metal and dielectric media, respectively.

For the optical excitation of surface plasmons, mostly prism and grating couplers are used to establish the phase-matching between an exciting light beam and surface plasmons. In SPR prism couplers relying on the attenuated total reflection method (ATR) with the Kretschmann geometry, a light beam is launched into a high refractive index glass prism (refractive index n_p) with a thin metal film (refractive index n_m) and a lower refractive index dielectric (refractive index $n_d < n_p$) on its base, see Fig. 2(a). The light beam is made incident at the prism base at the angle θ for which it is total internal reflected. Upon the total internal reflection, the light beam penetrates via its evanescent field into the thin metal film and reaches the outer interface between the metal and the lower refractive index dielectric. For a sufficiently high refractive index of the prism, the component of the

propagation constant of the light beam that is parallel to the surface $k_0 n_p \sin(\theta)$ can be matched to that of SP on the metal outer interface,

$$k_0 n_p \sin(\theta) = \text{Re}\{\beta\}, \quad (3)$$

where $\text{Re}\{\beta\}$ is the real part of the propagation constant of SP described by Eq. (1). As Fig. 2(b) shows, long range surface plasmons can be excited by using a prism coupler with a layer structure consisting of a dielectric buffer layer with refractive index n_b , a thin metal film, and a top dielectric with a refractive index n_d that is close to the one of the buffer layer $n_d \approx n_b$. Similarly, the coupling to LRSP can occur if its real part of the propagation constant $\text{Re}\{\beta\}$ that is described by Eq. (2) matches the parallel component of the propagation constant of the light beam $k_0 n_p \sin(\theta)$.

If the condition (3) holds, the coupling of the light beam to the surface plasmon modes can occur, which gives rise to a characteristic resonant dip in the spectrum of the reflected intensity, see Fig. 3(a). As shown in Fig. 3(b), the energy of the incident light beam is concentrated at the metallic surface upon the excitation of surface plasmon modes providing a strong enhancement of the intensity of the electromagnetic field. These simulations show that LRSPs are excited at lower angles compared to SPs due to their smaller real part of the propagation constant $\text{Re}\{\beta\}$. As the damping of LRSPs is lower than that of SPs, their excitation is accompanied with a narrower resonant dip and larger enhancement of the intensity of electromagnetic field $|E|^2$ on the metallic surface which can reach up to two orders of magnitude.

In the grating coupler, the diffraction on a periodically modulated surface is employed to enhance the propagation constant of a light beam to match that of a surface plasmon $\text{Re}\{\beta\}$. As seen in Fig. 4(a), a light beam propagating in a dielectric with a refractive index n_d is incident at a relief metallic grating with grooves perpendicular to the plane of incidence. Upon the incidence, the light beam is partially reflected and partially coupled to a series of diffracted waves. The component of the wave vector of a diffracted wave that is parallel to the grating surface is altered as follows:

$$k_{xp} = k_0 n_d \sin(\theta) + p \frac{2\pi}{\Lambda}, \quad (4)$$

where θ is the angle of incidence of the light beam, Λ is the period of the diffraction grating, and an integer p is the order of a diffracted wave. The parallel component of the propagation constant of a diffracted wave k_{xp} can be matched to the real part of the propagation constant of a SP guided along the metallic grating surface. For a shallow modulation of the grating, the SP propagation constant approximates that for a planar surface expressed by Eq. (1) and the coupling condition takes the form

$$k_0 n_d \sin(\theta) + p \frac{2\pi}{\Lambda} = \pm \text{Re}\{\beta\}. \quad (5)$$

Analogous to the prism coupler, the excitation of a SP wave on the surface of a metallic diffraction grating is manifested as a resonant dip (for the coupling through odd dif-

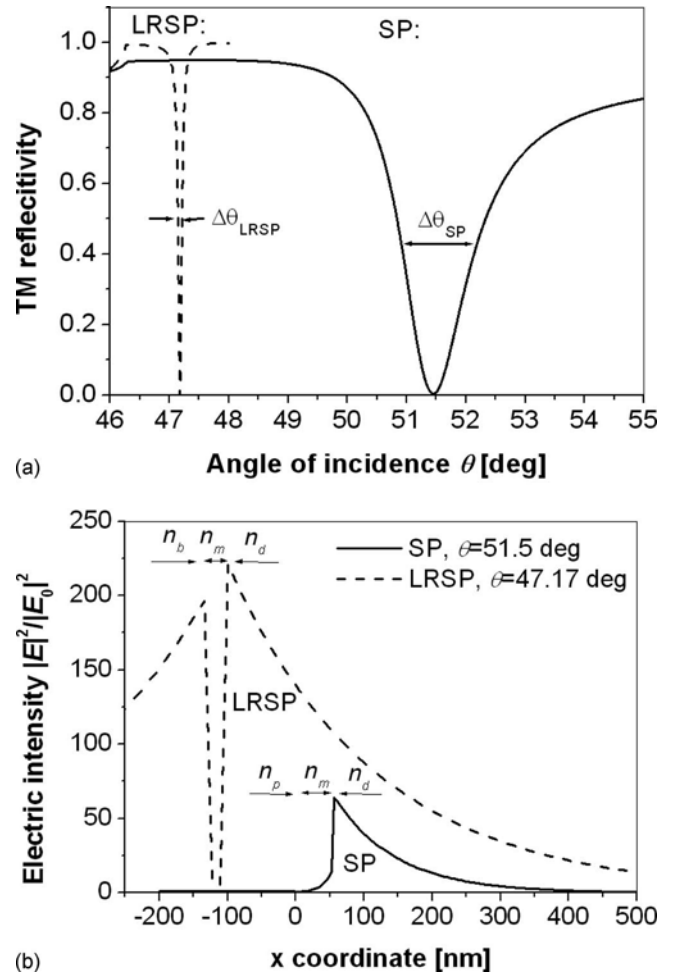


Fig. 3. Simulations of (a) angular reflectivity spectra and (b) the electric intensity field distribution for the prism coupling to SPs and LRSPs at the wavelength of $\lambda = 0.633 \mu\text{m}$. The following structure was assumed for the excitation of SPs: prism ($n_p = 1.845$), gold film ($n_m = 0.1 + 3.5i$ and $d_m = 55 \text{ nm}$), and a dielectric ($n_d = 1.333$). For the excitation of LRSP, the gold film was replaced by a buffer layer ($n_b = 1.340$, thickness of 900 nm) with gold film ($n_m = 0.1 + 3.5i$ and $d_m = 22.5 \text{ nm}$) on its top. The electric intensity distribution $|E|^2$ was normalized with that of the incident wave $|E_0|^2$.

fraction orders p) in the reflectivity spectrum and it is accompanied by the enhancement of intensity of electromagnetic field on the grating surface, see Fig. 4.

III. SURFACE PLASMON-ENHANCED FLUORESCENCE SPECTROSCOPY

A fluorophore is a molecule that can absorb a photon of a specific wavelength and re-emit it at another higher wavelength. As seen in the Jablonski diagram given in Fig. 5, upon the absorption the fluorophore is excited from its ground state S_0 to a higher singlet state S_1 , followed by the spontaneous relaxation. In a free space, the fluorophore can recombine back to the ground state S_0 by emitting another photon at a higher wavelength (radiative decay channel) or without emitting a photon, e.g., due to collisional quenching (nonradiative decay channel). The fluorescence emission rate of P_{em} depends on the excitation rate P_{ex} , the radiative decay rate P_r , and the nonradiative decay rate P_{nr} as

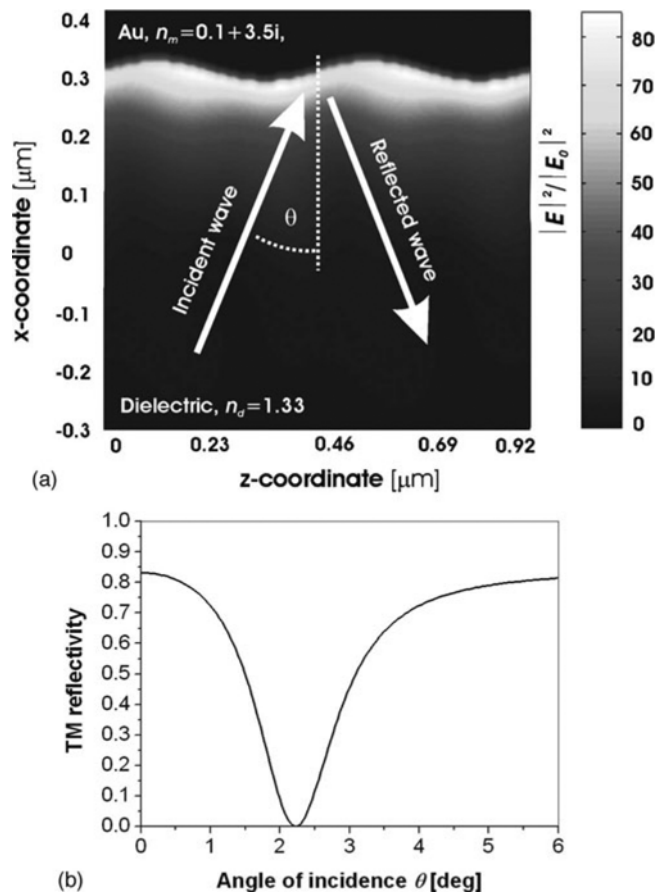


FIG. 4. Simulations of (a) distribution of electric intensity field and (b) angular reflectivity upon the excitation of SPs on a gold sinusoidal diffraction grating with the following parameters: gold with the refractive index of $n_m = 0.1 + 3.5i$ and a dielectric with the refractive index of $n_d = 1.33$, the grating period of $\Lambda = 455$ nm and the modulation depth of 35 nm, plus first diffraction order coupling ($p=1$) and the wavelength of $\lambda = 0.633$ μm . The electric intensity distribution $|E|^2$ was normalized with that of the incident wave in the prism $|E_0|^2$.

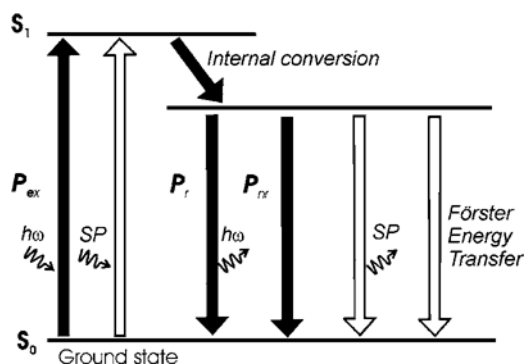


FIG. 5. Jablonski diagram showing transitions taking place within a fluorophore in a free space (black arrows) and additional excitation of decay channels occurring in the proximity to a metallic interface (black and white arrows).

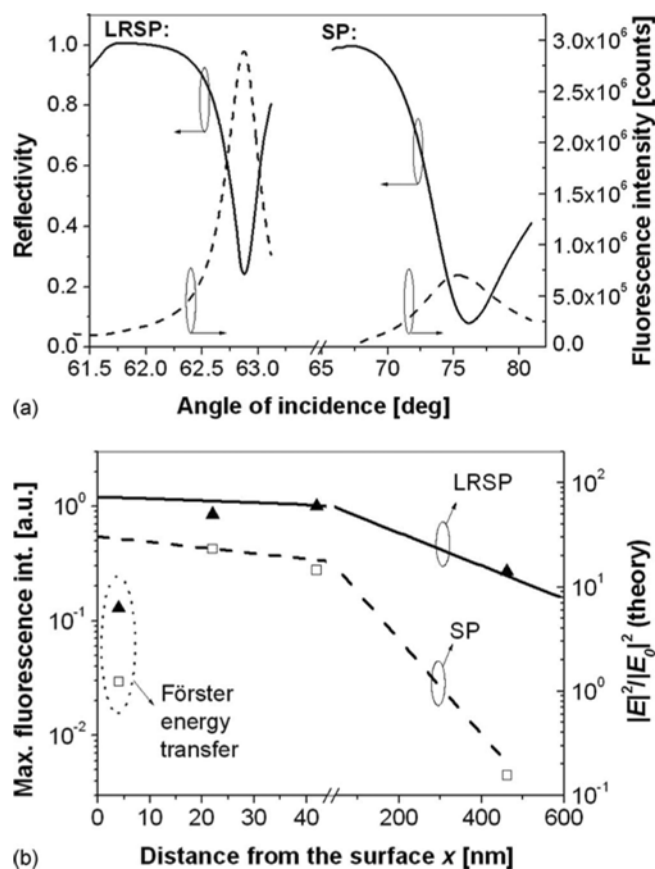


FIG. 6. Comparison of the fluorescence signal measured from a layer loaded with chromophore Alexa Fluor 647 that was probed with LRSPs and SPs: (a) angular reflectivity and fluorescence intensity spectra for the distance between chromophores and the metallic surface of 42 nm; (b) the dependence of the maximum fluorescence intensity on the distance between chromophores and the metallic surface.

$$P_{em} \propto P_{ex} \frac{P_r}{P_r + P_{nr}}. \quad (6)$$

Let us note that the quantum yield defined as $Q = P_r / (P_r + P_{nr})$ is in the range of 0.5–0.9 and the lifetime $\tau = (P_r + P_{nr})^{-1}$ is between 1 and 10 ns for most commonly used organic chromophores.

As Eq. (6) shows, the fluorophore emission rate P_{em} increases with the excitation rate P_{ex} . Far from the saturation, the excitation rate P_{ex} is proportional to the intensity of electromagnetic field at the absorption wavelength. Therefore, the emission rate P_{em} can be increased by placing a fluorophore within the enhanced intensity of surface plasmon field leading to higher intensity of emitted fluorescence light. This feature is illustrated in Fig. 6(a), which shows the angular reflectivity spectra measured upon the excitation of SP and LRSP and the accompanied intensity of fluorescence light emitted from a monolayer of chromophore-labeled molecules on a SPR active metallic surface. This figure reveals that the maximum fluorescence signal occurs upon the resonant coupling to surface plasmon modes. In addition, it shows that the peak fluorescence intensity measured upon

the chromophore excitation via LRSPs is larger than that obtained for the excitation through SPs.²³ Figure 6(b) shows the dependence of the fluorescence signal on the distance between the chromophore and the metallic surface. At distances larger than 40 nm, the fluorescence intensity exponentially decays from the metal surface due to the evanescent profile of surface plasmon field. LRSPs excite fluorophores more efficiently compared to SPs owing to the lower damping and more extended field profile.

If a fluorophore is placed in a close proximity to a metallic surface, besides the surface plasmon assisted excitation channel also two new decay channels are open, see Fig. 5. First, a nonradiative decay channel due to the Förster energy transfer between the fluorophore and electrons in a metal quenches the fluorescence signal at distances up to 10–15 nm. Second, a strong coupling of fluorescence light to surface plasmons occurs at distances up to several hundreds of nanometers from the metal surface.²⁴ On flat optically thick metal layers, these surface plasmons are not coupled with far field photons and thus the fluorescence light trapped in these modes is dissipated. However, this decay channel can be turned to be radiative by using an appropriate out-coupling scheme for surface plasmons. Diffraction grating couplers^{25,26} as well as prism couplers²⁴ were demonstrated to enable the recovering of fluorescence light that was emitted to surface plasmons. In addition, nanostructured metallic surfaces exhibiting a plasmonic bandgap at the emission wavelength of a fluorophore offers another possibility to reduce the dissipation of fluorescence light due to the coupling to surface plasmon modes.²⁷ Let us note that the interaction of a fluorophore with surface plasmons depends on the orientation of its dipole with respect to the metallic surface.²⁸ For illustration purposes we present in Fig. 7 the simulations performed by Calander,²⁹ showing the angular distribution of the intensity of the electromagnetic field emitted by a chromophore dipole oriented normal to a thin silver film on a glass prism. One can see that the coupling of the fluorescence light into surface plasmons and their subsequent out-coupling via the glass prism provides a highly directional fluorescence emission pattern.

In general, the interaction of fluorophores with surface plasmons enables the implementation of advanced schemes for fluorescence spectroscopy-based biosensors. First, the enhanced intensity of the electromagnetic field on a metallic surface associated with the resonant excitation of surface plasmon modes allows for orders of magnitude higher excitation rates P_{ex} which directly translates to an increase in the fluorescence signal.³⁰ Second, the fluorescence emission to surface plasmons and their subsequent out-coupling enables to control the angular emission pattern and thus to achieve higher yield in the fluorescence light detection.^{29,31} Third, the decreased lifetime of a chromophore in the vicinity to the metal³² was shown to suppress the photobleaching of organic chromophores.^{33,34}

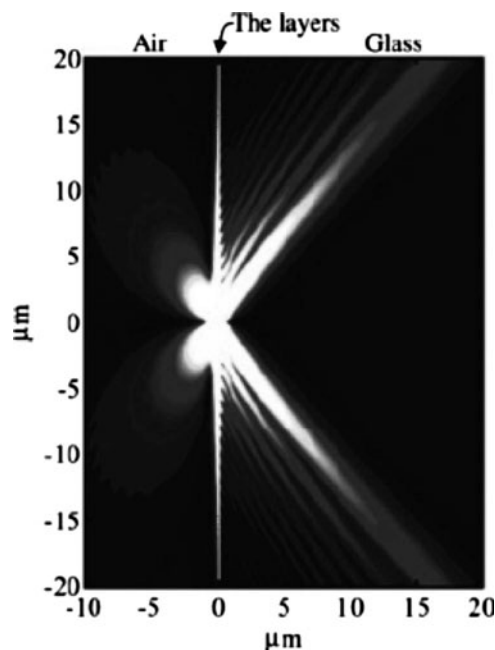


FIG. 7. Surface plasmon mediated fluorescence emission: simulations of the distribution of intensity of electromagnetic field emitted by a fluorophore deposited on a thin silver film with a dielectric spacer on the top of a glass prism. Reprinted with permission from Ref. 29. Copyright 2004 American Chemical Society.

IV. BIOSENSORS BASED ON SURFACE PLASMON-ENHANCED FLUORESCENCE SPECTROSCOPY

A. Optical platforms

The implementation of a biosensor utilizing SPFS was first reported by Attridge *et al.*³⁵ in early '90s of the last century and after a decade it was reintroduced in a simplified version by Lieberman and Knoll.⁹ Typically, a setup based on angular modulation of SPR is combined with fluorescence spectroscopy detection as shown in Fig. 8. A monochromatic laser beam is coupled to surface plasmons on a metallic sensor surface by using ATR method with the Kretschmann geometry. To the surface, biomolecular recognition elements are anchored for the specific capture of target molecules con-

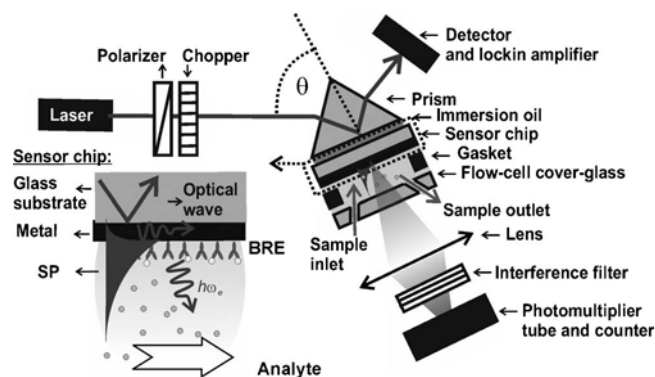


FIG. 8. An optical setup supporting a biosensor based on SPFS with SPR prism coupler and the angular modulation of SPR.

tained in a liquid sample that is flowed through a flow cell on its top. The target molecules are labeled with fluorophores of which absorption band matching the wavelength of the excitation laser beam. The enhanced intensity of the electromagnetic field that is associated with the coupling to surface plasmons provides an efficient excitation of fluorophore-labeled molecules adhered to the surface. Due to the evanescent profile of surface plasmon field, only molecules captured at the surface are excited while those contained in the bulk sample are not. The fluorescence light emitted from the sensor surface passes through the transparent flow cell, is collected by a lens, and its intensity is measured by a photomultiplier. In order to suppress the background signal due to the scattering of the light beam at the excitation wavelength, a band-pass filter with the transmission window at the fluorophore emission wavelength is mounted after the lens for collecting the fluorescence light. By using this setup, the binding of fluorophore-labeled molecules to the sensor surface is observed as a strong peak in the angular fluorescence spectrum [see Fig. 6(a)]. The maximum fluorescence signal which occurs upon the resonant coupling to SPs can be measured as a function of time which enables the monitoring kinetics of biomolecular reactions on the sensor surface.

A laser beam with a wavelength λ in the red or near infrared part of spectrum is often used for the excitation of surface plasmons in SPFS-based biosensors due to the availability of many organic chromophore labels with absorption band in this spectral region. For these wavelengths, a thin SPR active gold film is typically deposited on the sensor surface by, e.g., sputtering or thermal evaporation. In SPFS biosensors, gold SPR active coatings offer the advantage of good chemical stability, large enhancement of electromagnetic field upon the coupling to surface plasmons, and numerous surface chemistries for attaching biomolecular recognition elements available. In order to excite fluorophores with the absorption band at lower wavelengths, a layer structure consisting of a thin silver film and a gold overlayer (thickness of several nanometers) was used. For example, such structure allows for an efficient excitation of fluorophore labels at the wavelength $\lambda = 543$ nm via the enhanced field of surface plasmons.^{36,37} Another layer structure consisting of 50 nm thick silver layer and a 5 nm silicon dioxide film was used for the SPFS with the excitation wavelength of $\lambda = 532$ nm.³⁸ Recently, the SPFS technique was combined with the excitation of long range surface plasmon modes (LRSPs).^{23,39} The excitation of LRSPs can occur in a refractive index symmetrical structure and it provides higher enhancement of electromagnetic field compared to conventional surface plasmons. For the prism coupling to LRSPs, a layer structure consisting of a low-refractive index buffer layer, thin gold film, and an aqueous sample was used. The low-refractive index buffer layers were prepared from Teflon AF (from Dupont, Inc., USA, refractive index of $n_b \approx 1.31$) and Cytop (from Asahi, Inc., Japan, $n_b \approx 1.34$) polymers which can be spin coated on the sensor surface.^{23,39}

In the implementation of SPFS-based biosensor promoted by Liebermann and Knoll,⁹ the coupling to surface plasmons

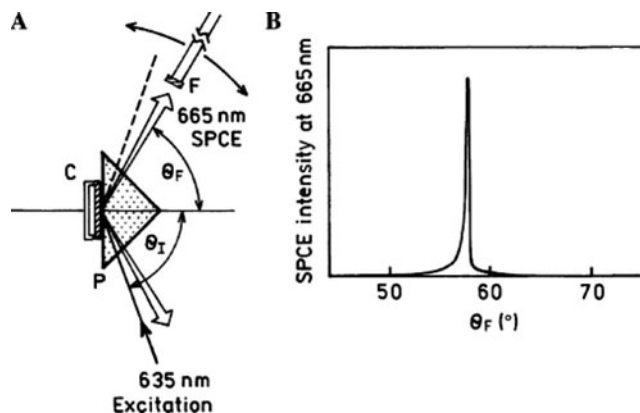


FIG. 9. (a) Scheme of an optical setup for prism out-coupling of the fluorescence light emitted to surface plasmons and its collecting by using an optical fiber (F). (b) The angular spectrum of the fluorescence light intensity measured upon the excitation of Alexa Fluor 647-labeled molecules deposited on the sensor surface at the emission wavelength of $0.665 \mu\text{m}$. Reprinted with permission from Ref. 41.

provides a strong enhancement of the excitation rate P_{ex} of labeled molecules captured on the sensor surface. However, a substantial portion of the fluorescence light is emitted to surface plasmon modes and does not reach the detector. In order to increase the efficiency in the fluorescence detection, the light emitted by fluorophores to surface plasmons can be recovered by surface plasmon out-coupling—a process inverse to surface plasmon excitation.^{25,26} The implementation of this approach to SPFS-based biosensor was reported only recently by Lakowicz and co-workers.^{40,41} In these works a SPR prism coupler served both for the excitation of adhered fluorophores and for the collecting of fluorescence light through out-coupling of surface plasmon at the emission wavelength, see Fig. 9. Moreover, Matveeva *et al.*⁴² showed that the out-coupling of fluorescence light emitted to surface plasmon offers an elegant way for color multiplexing of surface reactions. Because the out-coupling of surface plasmons occurs at distinct angles for different wavelengths, the fluorescence signal originating from the binding of molecules labeled with fluorophores exhibiting different emission wavelengths can be measured independently at separate angles.

For parallel detection of multiple reactions on the sensor surface, fluorescence spectroscopy was combined with surface plasmon microscopy.⁴³ In this approach, a large diameter laser beam was coupled to a SPR prism coupler to excite surface plasmons on the sensor chip area with an array of sensing spots. The spatial distribution of the fluorescence signal across the chip was measured by using imaging optics and a charge coupled device (CCD) detector. In addition, the color multiplexing was implemented into surface plasmon-enhanced fluorescence microscopy by using a color CCD camera and quantum dot labels exhibiting well defined distinct peaks in emission wavelength spectrum.³⁶

The relatively simple setup of SPFS-based sensor, which was originally used by Liebermann and Knoll,⁹ allows for the detection of the binding of ultrasmall amount of fluoro-

phores adhered to the sensor surface. From the data presented by Yu *et al.*,⁴⁴ one can estimate that a detectable fluorescence signal can be measured from as low as $\sim 10^{-3}$ fluorophores/ μm^2 . Moreover, the used optical configurations enables simultaneous detection of molecular binding through fluorescence signal (SPFS readout) as well as through induced refractive index changes (SPR readout). This feature can provide additional information on the investigated interactions^{45–47} and can be used for the calibration of the fluorescence signal.⁴⁴

B. Surface architectures for immobilization of biomolecules

In contrast to SPR biosensors relying on the measurement of refractive index changes, their SPFS counterparts do not exhibit the highest sensitivity to biomolecular binding that occurs directly at the metallic sensor surface. The optimum distance between a fluorophore and a metallic surface providing maximum fluorescence signal was experimentally determined to be approximately 30 nm. At this distance, the effects of the exponential decay of the SP electromagnetic field intensity and the Förster energy transfer quenching are balanced.³¹ Therefore, the design of a surface architecture (and detection assay) should provide a spacer of a similar thickness between the metal and captured fluorophore-labeled molecules.

For the immobilization of DNA or PNA probes, mostly mixed thiol self-assembled monolayers (SAMs) with biotin moieties were deposited on a gold sensor surface and the biotinylated probes were subsequently attached by using avidin or streptavidin linkers.^{14,48} An alternative approach based on the immobilization of DNA probes into a plasma polymerized allylamine network was shown to provide similar performance as this two-dimensional architecture.⁴⁹ Protein catcher molecules were typically immobilized by using the active ester chemistry to a gold surface modified by thiol SAM with carboxylic groups⁵⁰ or by using biotin-streptavidin chemistry to a surface with biotin terminated thiol SAM.⁵⁰ In addition, the incorporation of proteins into phospholipid bilayers tethered to a metal surface was reported.^{47,51,52} In order to prevent the fluorescence quenching and to exploit the whole evanescent field of surface plasmons for the excitation of fluorophores, a three-dimensional binding matrices based on a dextran brush were used for the immobilization of protein^{44,53} and DNA (Ref. 54) catcher molecules. For parallel detection of multiple DNA hybridization events, spotting of the DNA probes on the sensor surface was performed^{36,43} and electrochemically addressable deposition of DNA arrays was developed.³⁷

C. Labeling of biomolecules with fluorophores

As fluorescent labels, mostly organic dye molecules are employed. Typically, dye molecules with an absorption band in the red and near infrared part of the spectrum (e.g., Cy5) are employed as at these wavelengths surface plasmons can be easily excited on most commonly used gold surfaces. Analyte molecules can be labeled with organic fluorophores

either enzymatically (DNA by using labeled primers for the polymerase chain reaction) or through a chemical reaction (proteins). One of the main drawbacks of organic fluorescent dye molecules is their photobleaching, which limits the number of possible excitation-emission cycles. Recently, quantum dots were introduced to SPFS-based biosensors.³⁶ These novel labels offer better photostability compared to organic fluorophores. Quantum dots exhibit a broad absorption band in the UV part of the spectrum and a narrow well defined emission band at a wavelength which can be tuned by their size. However, an effect referred to as blinking was reported^{55,56} which complicates the binding analysis.⁵⁶

D. Analysis of oligonucleotides

Surface plasmon-enhanced fluorescence spectroscopy provides a highly sensitive platform for the analysis of interactions of DNA.⁵⁷ Yao *et al.*¹⁴ demonstrated the detection of trace amounts of polymerase chain reaction amplicons with the limit of detection of 500 fM. In this work, DNA probes were attached to the sensor surface through streptavidin-biotin surface chemistry. By using the same surface chemistry and peptide nucleic acid (PNA) probes, fivefold reduced limit of detection of 100 fM was reported.¹⁴ Moreover, SPFS was proved to be a suitable technique for the measurement of kinetic parameters of DNA hybridization by Yu *et al.*,⁵⁸ who showed that the determined kinetic binding constants are identical to those obtained by label-free SPR biosensors.

By using SPFS, extensive investigation of mismatched DNA interactions was performed in order to develop a sensitive platform for the detection of mutations. For instance, Lieberman *et al.*⁵⁷ investigated the effect of different mismatched base pairs to the stability of DNA duplexes. They demonstrated that T-G mismatched base pairs produce a more stable duplex than the T-C base pair mismatches. Tawa and Knoll⁵⁹ found that a double stranded DNA is more destabilized if the mismatched base pair between the captured DNA strand and the anchored DNA probe is located farther away from the solid sensor surface. For PNA probes, affinity binding constants for the interaction with mismatched DNA monomers were measured by Park *et al.*⁶⁰ This work demonstrated possible discrimination of mismatches in analyzed DNA samples. A single base mismatch in a 15-mer DNA decreased the affinity constant for the binding to a 15-mer PNA probe by two orders of magnitude, see Fig. 10. Afterward, Tawa *et al.*⁶¹ investigated the implementation of this approach for the detection of DNA mutations in a mixture of target molecules.

In addition to high sensitivity, optical setups supporting SPFS-based biosensors allow for the simultaneous label-free (SPR) and fluorescence-based (SPFS) observation of events occurring on the sensor surface. To Stengel and Knoll,⁴⁵ this feature enabled the study of the elongation of DNA molecules by the action of DNA polymerase I. In their work, single stranded DNA molecules were immobilized to the sensor surface by streptavidin-biotin surface chemistry and their interaction with the DNA polymerase I and a mixture of deoxynucleotidetriphosphates was monitored. The combina-

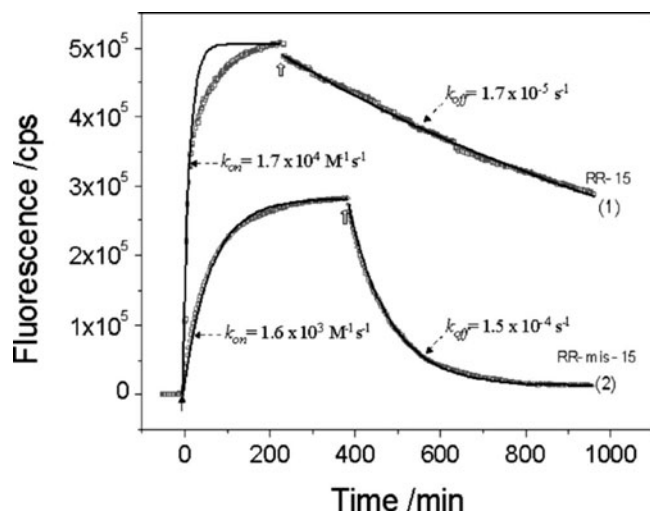


FIG. 10. Measured hybridization kinetics for the binding of DNA 15-mer molecules with complementary bases (1) and with a single mismatch (2) to PNA probes on the sensor surface. The kinetics was fitted with Langmuir model to determine the association and dissociation affinity binding constants k_{on} and k_{off} , respectively. Reprinted with permission from Ref. 60.

tion of SPR and SPFS allowed for the discrimination of the sensor response due to the incorporation of DNA polymerase I enzyme, the oligonucleotide elongation, and the release of the enzyme. The separation of response due to enzyme binding and enzyme activity allowed for the simultaneous measurement of binding and catalytic constants for this reaction.

SPFS-based biosensors for the analysis of DNA interactions were combined with an array detection format by using surface plasmon-enhanced fluorescence microscopy.^{36,43} The potential of this approach for high-throughput analysis of DNA interactions was demonstrated by Lieberman and Knoll.⁴³ In this work, the interactions of three different DNA molecules and three different probes spotted on the sensor surface were investigated. Samples with different chromophore-labeled DNA molecules were sequentially injected to the sensor with an array of DNA probes and the kinetic parameters for each reaction were simultaneously determined. Lately, Robelek *et al.*³⁶ explored the possibility to extend the SP-enhanced microscopy by employing the spectrometry. These authors showed that the spectrometry enables the implementation of color multiplexing of surface reactions. To each DNA analyte, quantum dot labels with specific emission band were attached. These quantum dot labels were excited at the same wavelength of $\lambda=543$ nm and the spatial distribution and wavelength spectra of the fluorescence light were measured. The measurement of the fluorescence light spectra upon the injection of a mixture of all DNA analytes enabled the binding monitoring for each combination of target molecule-probe simultaneously.

E. Analysis of membrane proteins

The biosensor platform enabling the simultaneous monitoring of refractive index changes (SPR) and fluorescence signal (SPFS) was applied for the investigation of membrane proteins embedded in biomimetic lipid layers.^{47,51,52} In these

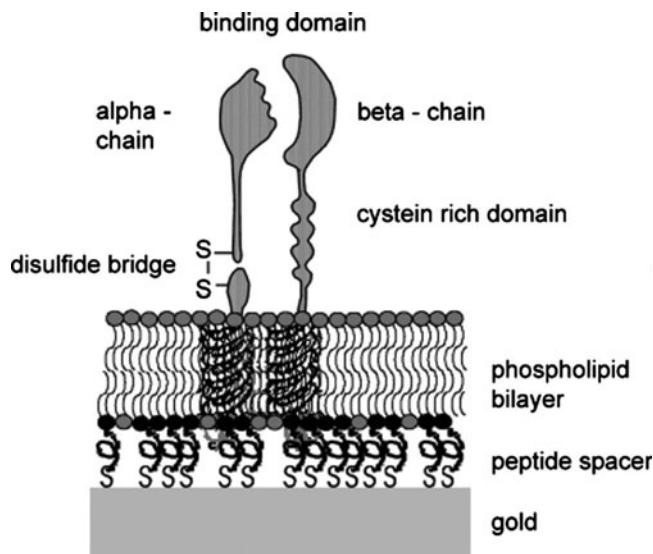


FIG. 11. Scheme of an integrin receptor molecule incorporated into a peptide-tethered lipid membrane. Reprinted with permission from Ref. 47.

applications, the formation of planar lipid membranes was observed by SPR via induced refractive index changes and the activity of incorporated membrane proteins was tested by SPFS method. Schmidt *et al.*⁶² investigated the immobilization of the acetylcholine receptor (AChR) ion channels into a thiopeptide-lipid monolayer. The incorporation and proper orientation of AChR proteins were monitored by the SPFS detection of the binding of specific fluorophore-labeled antibodies. Afterwards, the formation of artificial peptide-supported lipid bilayers and the incorporation of integrin transmembrane receptors $\alpha_v\beta_3$ and $\alpha_1\beta_1$ by vesicle spreading was investigated, see Fig. 11. By using similar biomimetic system, Sinner *et al.*⁴⁷ studied the orientation and accessibility of incorporated integrins by the SPFS detection of binding of specific antibodies. They demonstrated that integrins retained their biological functionality through the SPFS observation of their interaction with natural ligands. Later, Lössner *et al.*⁵¹ extended these studies by the investigation of the interaction of integrins with synthetic mono- and oligomeric RGD-based (Arg-Gly-Asp) peptides and peptidomimetics. Williams *et al.*⁶³ explored the interaction of the membrane-lysing enzyme phospholipase with phospholipid bilayers immobilized to the surface. The enzyme binding and vesicle lysis were observed through SPR and the permeabilization by SPFS measurements, respectively.

F. Immunoassay-based biosensors

Research has been carried out toward the implementation of SPFS to immunoassay-based biosensors over the last years. Vareiro *et al.*⁵⁰ investigated the efficiency of the capture of target molecules on a sensor surface depending on the orientation of anchored antibody receptors. They measured the binding of human chorionic gonadotropin (hCG) contained in a buffer to the antibodies against β subunit of hCG which were attached to the surface. These antibodies were

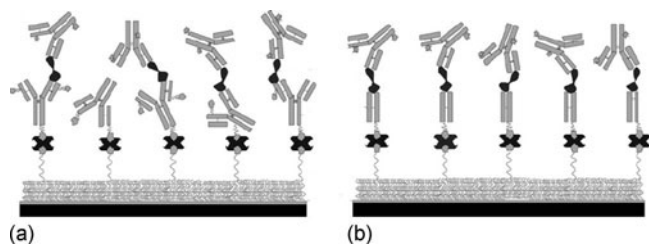


FIG. 12. Schematic representation of sandwich immunoassay for detection of hCG: (a) sensor surface with randomly biotinylated antibody and (b) sensor surface with Fab-hCG monobiotinylated fragment. Reprinted with permission from Ref. 50. Copyright 2005 American Chemical Society.

labeled with a biotin and were coupled to biotin moieties on the surface by using a streptavidin linker. The IgG antibodies with randomly distributed biotin labels [see Fig. 12(a)] and monobiotinylated Fab fragments [see Fig. 12(b)] were tested. Using the sandwich assay and fluorescence dye-labeled secondary antibodies, the limit of detection of hCG reaching 4 pM (0.2 ng ml^{-1}) was obtained when antibody receptors were randomly oriented. By using the ordered monobiotinylated Fab fragments on the sensor surface, the limit of detection was improved to 0.6 pM (30 pg ml^{-1}). The detection of hCG was performed in cycles by using the regeneration of the sensor surface with 10 mM glycine-HCl buffer. Each detection cycle was shorter than 60 min.

Yu *et al.*⁴⁴ developed an immunosensor utilizing a three-dimensional binding matrix for the immobilization of receptors. In SPFS-based biosensors, this surface architecture offers two key advantages. First, a three-dimensional binding matrix provides a high binding capacity. Second, the binding of chromophore molecules can occur within the whole evanescent field of the surface plasmon at distances where fluorescence quenching does not occur. In the work of Yu *et al.*,⁶⁴ CM5 chip (commercially available from Biacore, Inc., Sweden) with a dextran brush was used for the immobilization of α -IgG catcher molecules by using active ester chemistry. This surface architecture in conjunction with SPFS allowed for highly sensitive detection of Alexa Fluor 647-labeled IgG molecules with the limit of detection of 0.5 fM. In these experiments, the detection was performed in a buffer solution and the incubation time was approximately 2 h. Afterward, this approach was implemented in a biosensor for the detection of free prostate specific antigen (*f*-PSA) in human plasma.⁵³ As illustrated in Fig. 13(a), a sandwich immunoassay was used for the detection of this prostate cancer marker. For the detection in human plasma, the nonspecific binding to the negative charged dextran brush at the surface was greatly reduced by spiking the samples with a negatively charged carboxymethyl dextran. The biosensor was possible to regenerate for repeated use and it was capable of *f*-PSA detection at concentrations of as low as 80 fM (2 pg ml^{-1}) after 40 min flow of a sample through the sensor.

An optical setup, which utilized surface plasmon-enhanced excitation of chromophores and the out-coupling of fluorescence light emitted to surface plasmons (surface plasmon coupled emission—SPCE) by a prism coupler, was

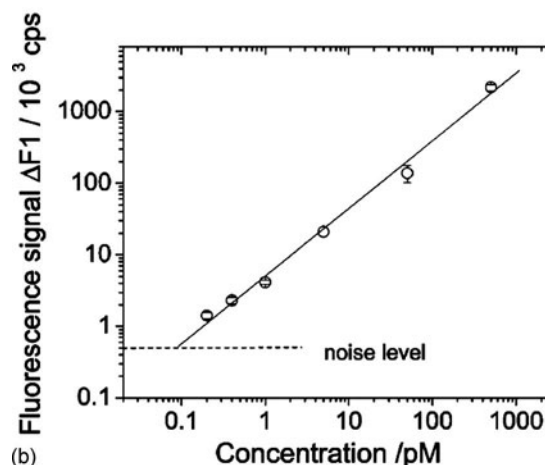
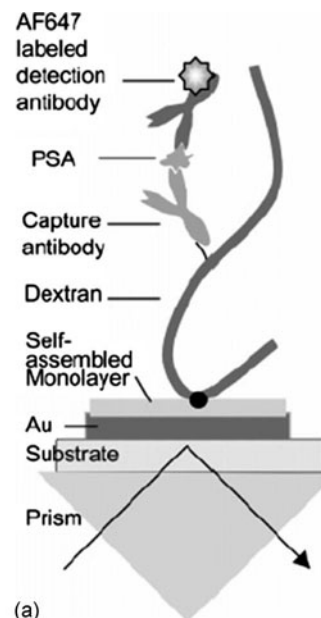


FIG. 13. (a) Schematic of SPFS-based sandwich *f*-PSA assay and a dextran binding matrix. (b) Calibration curve for the *f*-PSA detection in the plasma. Reprinted with permission from Ref. 53. Copyright 2004 American Chemical Society.

implemented in an immunosensor, see Fig. 9. By using SPCE method, the immunoassay-based detection in serum and whole blood samples was investigated by Matveeva *et al.*⁴¹ These authors nonspecifically adsorbed IgG molecules to the sensor surface and measured the capture of chromophore-labeled α -IgG antibodies from the whole blood samples at concentrations down to 10 nM ($0.15 \text{ } \mu\text{g ml}^{-1}$). Similar technique was used for the detection of myoglobin by using sandwich immunoassay.³⁸ In this biosensor, the detection assay included 1–2 h incubation of myoglobin sample with the sensor surface and the limit of detection of 3 nM (50 ng ml^{-1}) was achieved for this cardiac marker.

Only recently, the SPFS technique was combined with the excitation of special surface plasmon modes referred to as LRSPs which allows for higher enhancement of electromagnetic field intensity compared to conventional surface plasmons.^{23,39} The LRSP-enhanced fluorescence spectroscopy

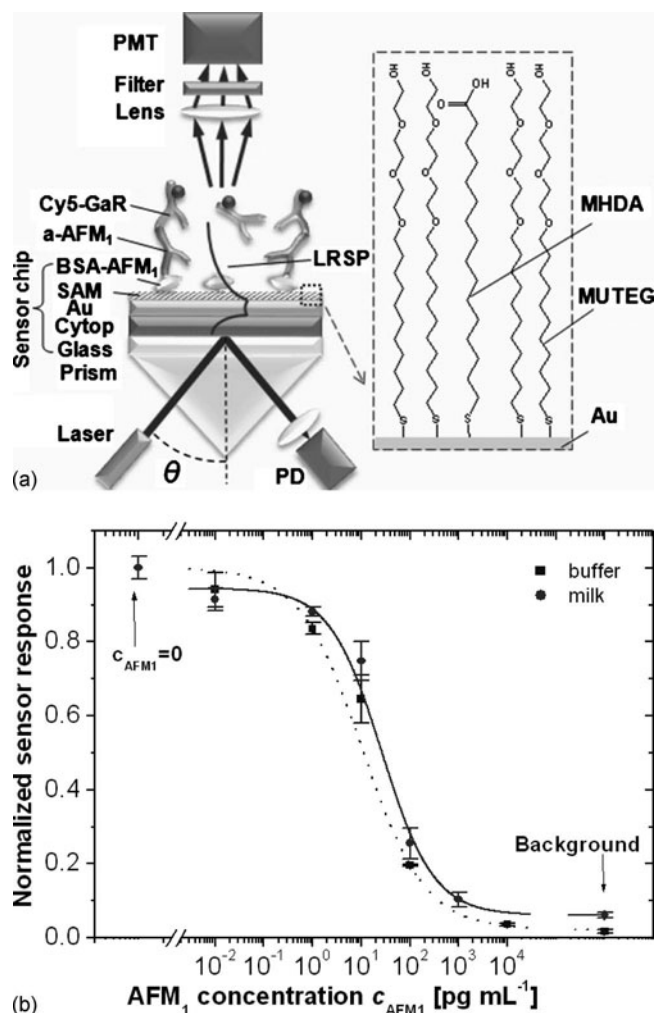


FIG. 14. (a) Schematic of a LRSP-enhanced fluorescence spectroscopy for the detection of aflatoxin M_1 (AFM_1) in milk by using an inhibition immunoassay. (b) Measured calibration curve for AFM_1 detection in buffer and milk samples.

copy was applied for the detection of aflatoxin M_1 (AFM_1) in milk samples by Yi *et al.*⁶⁵ By using inhibition competitive immunoassay, the limit of detection of 1.8 pM (0.6 pg mL^{-1}) was achieved. The scheme of the sensor assay and the calibration curve are depicted in Fig. 14. The analysis of a milk sample was performed in 53 min including its centrifuging, the incubation with specific antibody, and the detection of unreacted antibody captured on a sensor surface that was modified with the conjugate of bovine serum albumin and AFM_1 .

V. SUMMARY AND OUTLOOK

Over the past two decades, extensive research has been devoted to surface plasmon mediated fluorescence. This work paved the way toward the development of variety of biosensors exploiting on surface SPFS as described in this review. This method offers the advantage of ultrahigh sensitivity (detection of subfemtomolar concentrations of target analytes is possible), relative simplicity, and compatibility with label-free SPR biosensors. Since the introduction of

SPFS to SPR-based biosensors in the beginning of this decade, various optical configurations, techniques for multiplexing of sensing channels, and surface chemistries were developed. The applications of SPFS biosensors range from biomolecular interaction analysis to immunoassay-based detection of chemical and biological analytes. In the future, we envision a growing number of studies taking advantage of the combined label-free and the SPFS-based observation of biomolecular interactions. In addition, the implementation of SPFS technique for ultrahigh sensitive biosensors needed in various important fields such as medical diagnostics and food control will very likely become reality.

ACKNOWLEDGMENTS

The authors gratefully acknowledge the financial support of the European Commission in the Communities 6th Framework Programme, Project TRACEBACK (Grant No. FOOD-CT-036300) coordinated by Tecnoalimenti. This work reflects the authors' views; the Community is not liable for any use that may be made of the information contained in this publication.

- ¹J. Homola, Chem. Rev. (Washington, D.C.) **108**, 462 (2008).
- ²R. L. Rich and D. G. Myszka, J. Mol. Recognit. **20**, 300 (2007).
- ³J. Homola, *Surface Plasmon Resonance Based Sensors* (Springer, New York, 2006).
- ⁴G. D. VanWiggeren, M. A. Bynum, J. P. Ertel, S. Jefferson, K. A. Robotti, E. P. Thrush, D. A. Baney, and K. P. Killeen, Sens. Actuators B **127**, 341 (2007).
- ⁵S. Slavik and J. Homola, Sens. Actuators B **123**, 10 (2007).
- ⁶L. He, M. D. Musick, S. R. Nicewarner, F. G. Salinas, S. J. Benkovic, M. J. Natan, and C. D. Keating, J. Am. Chem. Soc. **122**, 9071 (2000).
- ⁷A. W. Wark, H. J. Lee, A. J. Qavi, and R. M. Corn, Anal. Chem. **79**, 6697 (2007).
- ⁸Y. Li, H. J. Lee, and R. M. Corn, Anal. Chem. **79**, 1082 (2007).
- ⁹T. Liebermann and W. Knoll, Colloids Surf., A **171**, 115 (2000).
- ¹⁰K. S. Phillips and Q. Cheng, Anal. Bioanal. Chem. **387**, 1831 (2007).
- ¹¹S. P. Fang, H. J. Lee, A. W. Wark, and R. M. Corn, J. Am. Chem. Soc. **128**, 14044 (2006).
- ¹²H. Vaisocherova *et al.*, Biopolymers **82**, 394 (2006).
- ¹³X. D. Su, Y. J. Wu, R. Robelek, and W. Knoll, Langmuir **21**, 348 (2005).
- ¹⁴D. F. Yao, F. Yu, J. Y. Kim, J. Scholz, P. E. Nielsen, E. K. Sinner, and W. Knoll, Nucleic Acids Res. **32**, 177 (2004).
- ¹⁵T. Neumann, M. L. Johansson, D. Kambhampati, and W. Knoll, Adv. Funct. Mater. **12**, 575 (2002).
- ¹⁶C. R. Taitt, G. P. Anderson, and F. S. Ligler, Biosens. Bioelectron. **20**, 2470 (2005).
- ¹⁷H. P. Lehr, M. Reimann, A. Brandenburg, G. Sulz, and H. Klapproth, Anal. Chem. **75**, 2414 (2003).
- ¹⁸G. L. Duveneck, A. P. Abel, M. A. Bopp, G. M. Kresbach, and M. Ehrat, Anal. Chim. Acta **469**, 49 (2002).
- ¹⁹J. R. Lakowicz, Plasmonics **1**, 5 (2006).
- ²⁰M. E. Stewart, C. R. Anderton, L. B. Thompson, J. Maria, S. K. Gray, J. A. Rogers, and R. G. Nuzzo, Chem. Rev. (Washington, D.C.) **108**, 494 (2008).
- ²¹H. Rather, *Surface Plasmons on Smooth and Rough Surfaces and on Gratings* (Springer-Verlag, Berlin, 1983).
- ²²D. Sarid, Phys. Rev. Lett. **47**, 1927 (1981).
- ²³J. Dostálek, A. Kasry, and W. Knoll, Plasmonics **2**, 97 (2007).
- ²⁴W. H. Weber and C. F. Eagen, Opt. Lett. **4**, 236 (1979).
- ²⁵W. Knoll, M. R. Philpott, and J. D. Swalen, J. Chem. Phys. **75**, 4795 (1981).
- ²⁶S. C. Kitson, W. L. Barnes, and J. R. Sambles, Opt. Commun. **122**, 147 (1996).
- ²⁷S. C. Kitson, W. L. Barnes, and J. R. Sambles, Phys. Rev. B **52**, 11441 (1995).

- ²⁸F. D. Stefani, K. Vasilev, N. Bocchio, N. Stoyanova, and M. Kreiter, *Phys. Rev. Lett.* **94**, 023005 (2005).
- ²⁹N. Calander, *Anal. Chem.* **76**, 2168 (2004).
- ³⁰S. C. Kitson, W. L. Barnes, J. R. Sambles, and N. P. K. Cotter, *J. Mod. Opt.* **43**, 573 (1996).
- ³¹K. Vasilev, W. Knoll, and M. Kreiter, *J. Chem. Phys.* **120**, 3439 (2004).
- ³²R. M. Amos and W. L. Barnes, *Phys. Rev. B* **55**, 7249 (1997).
- ³³K. Vasilev, F. D. Stefani, V. Jacobsen, W. Knoll, and M. Kreiter, *J. Chem. Phys.* **120**, 6701 (2004).
- ³⁴Y. Fu and J. R. Lakowicz, *Plasmonics* **2**, 1 (2007).
- ³⁵J. W. Attridge, P. B. Daniels, J. K. Deacon, G. A. Robinson, and G. P. Davidson, *Biosens. Bioelectron.* **6**, 201 (1991).
- ³⁶R. Robelek, L. F. Niu, E. L. Schmid, and W. Knoll, *Anal. Chem.* **76**, 6160 (2004).
- ³⁷L. Niu and W. Knoll, *Anal. Chem.* **79**, 2695 (2007).
- ³⁸E. Matveeva, Z. Gryczynski, I. Gryczynski, J. Malicka, and J. R. Lakowicz, *Anal. Chem.* **76**, 6287 (2004).
- ³⁹A. Kasry and W. Knoll, *Appl. Phys. Lett.* **89**, 101106 (2006).
- ⁴⁰J. R. Lakowicz, J. Malicka, I. Gryczynski, and Z. Gryczynski, *Biochem. Biophys. Res. Commun.* **307**, 435 (2003).
- ⁴¹E. G. Matveeva, Z. Gryczynski, J. Malicka, J. Lukomska, S. Makowiec, K. W. Berndt, J. R. Lakowicz, and I. Gryczynski, *Anal. Biochem.* **344**, 161 (2005).
- ⁴²E. Matveeva, J. Malicka, I. Gryczynski, Z. Gryczynski, and J. R. Lakowicz, *Biochem. Biophys. Res. Commun.* **313**, 721 (2004).
- ⁴³T. Liebermann and W. Knoll, *Langmuir* **19**, 1567 (2003).
- ⁴⁴F. Yu, B. Persson, S. Lofas, and W. Knoll, *J. Am. Chem. Soc.* **126**, 8902 (2004).
- ⁴⁵G. Stengel and W. Knoll, *Nucleic Acids Res.* **33**, 69 (2005).
- ⁴⁶F. Xu, B. Persson, S. Lofas, and W. Knoll, *Langmuir* **22**, 3352 (2006).
- ⁴⁷E. K. Sinner, U. Reuning, F. N. Kok, B. Sacca, L. Moroder, W. Knoll, and D. Oesterhelt, *Anal. Biochem.* **333**, 216 (2004).
- ⁴⁸D. Kambhampati, P. E. Nielsen, and W. Knoll, *Biosens. Bioelectron.* **16**, 1109 (2001).
- ⁴⁹Z. Zhang, W. Knoll, R. Foerch, R. Holcomb, and D. Roitman, *Macromolecules* **38**, 1271 (2005).
- ⁵⁰M. L. M. Vareiro, J. Liu, W. Knoll, K. Zak, D. Williams, and A. T. A. Jenkins, *Anal. Chem.* **77**, 2426 (2005).
- ⁵¹D. Lössner *et al.*, *Anal. Chem.* **78**, 4524 (2006).
- ⁵²B. Wiltshi, W. Knoll, and E. K. Sinner, *Methods* **39**, 134 (2006).
- ⁵³F. Yu, B. Persson, S. Lofas, and W. Knoll, *Anal. Chem.* **76**, 6765 (2004).
- ⁵⁴N. Yang, X. D. Su, V. Tjong, and W. Knoll, *Biosens. Bioelectron.* **22**, 2700 (2007).
- ⁵⁵F. D. Stefani, W. Knoll, M. Kreiter, X. Zhong, and M. Y. Han, *Phys. Rev. B* **72**, 125304 (2005).
- ⁵⁶R. Robelek, F. D. Stefani, and W. Knoll, *Phys. Status Solidi A* **203**, 3468 (2006).
- ⁵⁷T. Liebermann, W. Knoll, P. Sluka, and R. Herrmann, *Colloids Surf., A* **169**, 337 (2000).
- ⁵⁸F. Yu, D. F. Yao, and W. Knoll, *Nucleic Acids Res.* **32**, e75 (2004).
- ⁵⁹K. Tawa and W. Knoll, *Nucleic Acids Res.* **32**, 2372 (2004).
- ⁶⁰H. Park, A. Germini, S. Sforza, R. Corradini, R. Marchelli, and W. Knoll, *BioInterphases* **1**, 113 (2006).
- ⁶¹K. Tawa, D. F. Yao, and W. Knoll, *Biosens. Bioelectron.* **21**, 322 (2005).
- ⁶²E. K. Schmidt *et al.*, *Biosens. Bioelectron.* **13**, 585 (1998).
- ⁶³T. L. Williams, M. Vareiro, and A. T. A. Jenkins, *Langmuir* **22**, 6473 (2006).
- ⁶⁴S. Löfås and B. Johnsson, *J. Chem. Soc., Chem. Commun.* **1990**, 1526.
- ⁶⁵Y. Wang, J. Dostalek, and W. Knoll (unpublished).